A three-dimensional regression model of the shoulder rhythm in a wide-ranging envelope of humeral postures

Gil Gonçalves
gil.goncalves@tecnico.ulisboa.pt
Instituto Superior Técnico, Universidade de Lisboa, Portugal
July 2021

ABSTRACT

The aim of this work is to develop regression models for the shoulder which predict the orientation of the clavicle and the scapula from the humeral orientation. It aims to extend these models to a wider envelope of arm postures than the one available in the literature. Two types of regression models are built: one using exclusively the humeral orientation as a predictor and another one which also uses anthropometry data as predictors.

An optoelectronic tracking system, complemented with inertial measurement units and an external frame, is used. Shoulder kinematics are assessed using a non-invasive procedure with cutaneous markers and a scapula locator. Regression equations are obtained for the two types of regression models. For the one which uses individual factors as predictor variables, multicollinearity is detected and thus a statistical processing is made. The models are validated using an independent dataset.

The model without individual factors shows a fit to the data in the range of the preceding literature. The models with individual factors show a better fit to the test dataset than the model without. The inclusion of individual factors has, however, varying results when predicting the validation dataset. This can be explained by the high multicollinearity found among the predictors. This causes the regression coefficients to be very sensitive to small changes in the model.

Keywords: Shoulder; Kinematics; Scapulo-humeral rhythm; Shoulder rhythm; Regression model.

1 INTRODUCTION

The shoulder is, from a biomechanical standpoint, the most complex structure in the human body. It is also the most mobile joint in the body, relying on an intricate system that allows motion in six degrees of freedom. It is comprised of four joints. The rounded humeral head articulates with the glenoid cavity of the scapula, forming the glenohumeral joint. The acromioclavicular joint is formed by the junction of the lateral clavicle and the acromion process of the scapula. The sternoclavicular joint results from the articulation of the medial aspect of the clavicle with the manubrium of the sternum. Finally, the scapulothoracic joint, which is not a true anatomic joint, since it does not display the usual joint characteristics, i.e., union by fibrous, cartilaginous, or synovial tissues, is formed by the articulation of the scapula with the thorax. The shoulder joint plays an important role in many daily activities as well as in sports performances.

It is composed of three bones, the clavicle, the scapula, and the humerus. Together they form a kinematic chain: during movement of the upper limb a defined relation between their individual motions has been observed (Hogfors et al., 1991; Inman et al., 1944). This movement pattern has been called the shoulder rhythm (De Groot & Brand, 2001; Grewal & Dickerson, 2013; Xu et al., 2014a). Assessing the orientation of the shoulder girdle bones using in vivo non-invasive methods can be difficult due to the soft tissue overlying the bones (Brochard et al., 2011; Karduna et al., 2001; Prinold et al., 2011; van Andel et al., 2009). Nowadays, the application of a scapula locator is considered the optimum method for non-invasively tracking the movement of the scapula (Meskers et al., 2007). Static measurements using this device are found to provide more accurate data when compared to a dynamic acquisition, as the mismatches due to skin deformation are minimized (van Andel et al., 2009). Some studies have taken a regression-based shoulder rhythm approach (Hogfors et al., 1991; De Groot & Brand, 2001; Grewal & Dickerson, 2013), using the more easily measurable humeral orientation to estimate the orientations of the scapula and clavicle. Some of these studies also consider readily available anthropometric factors as covariates in the regression process. This results in a set of regression equations that help define the shoulder rhythm. However, these regression equations tables have a limited range of application due to the considered envelope of arm postures. Extrapolating shoulder rhythms to an

untested range may result in poor prediction of the scapula and clavicle orientation (Xu et al., 2014a).

In this work 3-D shoulder rhythm regression model are extended to a wider envelope of arm postures. Past studies have neglected arm postures in negative planes of elevation. To do so, an optoelectronic tracking system, complemented with inertial measurement units (IMU) and an external frame, is used to acquire shoulder kinematics. This external frame is built with the goal of improving the consistency of arm positioning and the comfort of the subjects. Shoulder kinematics are assessed using a non-invasive procedure with cutaneous markers and a scapula locator to help determine the locations of three scapula landmarks simultaneously. This scapula locator is 3-D printed to reduce the inaccuracies that arise relating to the placement of markers or soft tissue displacement. Two types of regression models are built to predict the 3-D orientations of the clavicle and scapula. The first model uses exclusively the humerus orientation as a predictor. The other two regression models use as input the humerus orientation as well as readily available anthropometry data as predictors. The regression models are validated using an independent dataset.

2 METHODS

2.1 Data acquisition

The present work focuses on the relationship between the movement of the humerus, the clavicle and the scapula. To study it 12 right-hand-dominant subjects (6 females and 6 males, 26.4 years ± 9.8, height: 1.72 ± 0.1 cm; weight: 66.1 ± 10.5 kg) with no acute or chronic upper extremity musculoskeletal disorders are recruited. Their anthropometrical data are represented in Table 1. The 3D-kinematics of the shoulder rhythm are collected using the precision motion capture and 3-D positioning tracking system Qualysis Tracking Manager (QTM), at the Lisbon Biomechanics Laboratory (LBL). It utilizes 14 digital infrared cameras interacting with 22 retro-reflective markers and one marker cluster per arm. The retro-reflective markers are attached to the bony landmarks of the thorax, clavicle, scapula, humerus and forearm, of each subject's right arm. The shoulder is tracked in a series of static arm postures in five elevation planes (-90º, -60º, -30º, 0º, 45º and 90º), five elevation angles (0º, 40º, 80º,120º,160º) and in three humeral axial rotation configurations (maximum internal, neutral and maximum external). The arm is kept straight in all tested postures. The data acquisition includes the usage of an external frame, a scapula locator and inertial measurement units, as detailed in Sections 2.2, 2.3 and 2.4, respectively.

Table 1: Average anthropometry data for the 12 subjects that participated in this study

Anthropometry Data	Definition	Average (mm)	SD (mm)
Length Thorax	IJ-PX	191.2732	26.5123
Depth Thorax	PX-T8	237.2062	21.6918
Length Clavicle	SC-AC	155.3850	13.0864
Length Scapular Spine	AA-TS	127.2294	10.8616
Length Scapula	AA-AI	189.3719	14.5157
Upper Arm Length	AC-EL	347.2010	16.2983

2.2 External Frame

The external frame aims at standardizing and supporting arm posture. It consists of a vertical support in the shape of a "question mark". The arc has an amplitude of 180º and a radius of 22 cm and is located at the end of a linear 78 cm segment. The discretized elevation angles are painted on the frame's arc. The vertical support is fixed (encastre) in a 30x1.8x10 cm wood platform, stabilized by two blocks. This platform is allowed to rotate around the axis of a 20 cm steel screw, fixed (encastre) in a panel laid on the floor. This rotation allows the entire vertical frame to rotate to the selected thoracohumeral elevation plane, painted on the floor panel. The participant has to be aligned with the centre of the external frame, in order to correctly attain each humeral. For the more uncomfortable postures an extra frame (Figure 1b) is set next to the participant's left arm to provide extra support and minimize lateral flexion of the thorax.

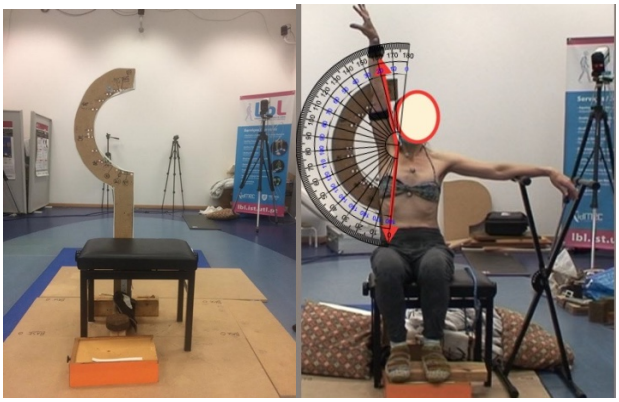

(a) (b)

Figure 1: (a) Overview of the built external frame; (b) Data acquisition for a humeral posture in the 0º elevation plane and with 160º elevation angle and maximum internal rotation, with the aid of the two external frames. The digitally superimposed protractor has the goal of visually estimating the joint elevation angle and assuring it matched the given frame elevation angle

2.3 Scapula Locator

The scapula locator is designed using *SolidWorks* and then 3-D printed. This three-rod device uses the two adjustable beams to locate the positions of the scapula's angulus acromialis, trigonum spinae, and angulus inferior. After adjusted to the individual scapula, the rods are fixed into a rigid triangular position. At each new position, the scapula locator is readjusted to the bony landmarks of the scapula and a new recording is made. After 9 designs with various flexion angles, thicknesses, lengths and edges profiles, the final design, shown in Figure 2, is reached. The two segments of the scapula locator are printed with a 17º degree of curvature to better adjust to the natural curvature of the participant's scapula region. This value is chosen following the average curvature of the upper thoracic spine of 16.5º (Wakimoto et al., 2018). The corners of the apparatus are rounded to improve ergonomics.

2.4 Inertial Measurement Units

A wireless inertial sensor system Biosyn's F.A.B. System-Functional Assessment of Biomechanics, from Biosyn, Canada, is used. The IMU are placed over the skin or clothes using elastic bands. The sensor data are transmitted to a receiver (F.A.B Belt Clip receiver) and then to the computer to which it is connected. Here, an avatar is animated and displayed in real time, providing immediate visual feedback. This helps detect thorax tilts and the need to readjust the participant's posture or the bench's height. These sensors also estimated in real time the humeral axial rotation, which allowed the participant to be directed to the neutral axial rotation. The sensors also estimated the thoracohumeral joint's elevation angle before kinematic data were processed.

2.5 Data Analysis

For each arm posture, joint angles are calculated using software developed in-house (Quental et al., 2015, 2018) and coded in MATLAB (Mathworks, Natick, MA). Joint angles are calculated using the three-dimensional coordinates of relevant markers. The glenohumeral joint centre is estimated using the algorithm of Gamage & Lasenby (2002). The thoracohumeral joint, scapulothoracic joint and the sternoclavicular joint angles are decomposed using the Euler angle sequence recommended by the ISB (Wu et al., 2005) (Table 2).

Table 2: Euler decomposition orders and their interpretations according to ISB standards (Wu et al., 2005) describing the orientation of clavicle, scapula, and humerus orientation with respect to the thorax.

Joint	Euler decomposition order	Rotation description	Designation
Sternoclavicular	Y X	Retraction/protraction Elevation/depression	SC1 SC2
Scapulothoracic	Y X Z	Retraction/protraction Lateral/medial rotation Anterior/posterior tilt	ST1 ST2 ST3
Thoracohumeral	Y X Y	Plane of elevation Elevation Axial rotation	HT1 HT2 HT3

2.6 Regression Models

Out of the 12 subjects (6 females and 6 males), 4 females and 4 males (age: 27.8 ± 12.0 years, height: 1.72 ± 0.04 m, weight: 66.4 ± 9.5 kg) are randomly selected to build the regression models. Two types of regression models are computed: the first type included only the three thoracohumeral angles as predictor variables; and the second type included the three thoracohumeral angles as well as a selection of individual factors as predictors. Each regression model is built through a two-step regression process, in agreement with previous studies (de Groot and Brand, 2001; Grewal and Dickerson, 2013; Xu et al., 2014a). In the first step, all predictors are centred to reduce multicollinearity (Aiken et al., 1991) and the *z*-score of each variable's measurement is calculated. The three thoracohumeral angles are treated as continuous variables, and, in the models that included individual factors, gender is treated as a nominal variable while the remaining individual factors are treated as continuous variables. A linear regression model is used to assess the influence of the independent variables, detailing the p-value for each variable and defining the significant variables. In the second step, the significant variables from the first step are treated as continuous variables to build the regression equation by forward and backward stepwise regression. For the stepwise regression, the p-value required for a term to be entered in the model (i.e. considered a predictor variable) is 0.05, and the p-value for a term to be retained in the model is 0.10. In previous studies (Grewal and Dickerson, 2013; Xu et al., 2014a), only the thoracohumeral angles, if deemed significant in the first step, had their quadratic and interaction terms evaluated in the second step. In this study, this analysis is extended to all significant variables, in order to better understand the influence of individual factors on the shoulder rhythm as well as the dependency between predictor variables. The output model may contain an intercept, linear and squared terms for each significant predictor, and all products of pairs of significant distinct predictors.

Three regression models are developed: Model 0 (M0), Model 1 (M1) and Model 2 (M2). Model 0 includes only the three thoracohumeral angles as predictor variables. Model 1 includes as predictors the three thoracohumeral parameters plus a comprehensive set of 10 individual factors: gender, age, height, weight, thorax length, thorax depth, clavicular length, scapular spine length, scapular length, upper arm length. The anthropometric data includes segments that are constrained by their relation in a closed chain mechanism. If predictors are correlated among themselves, multicollinearity is said to exist among them. Correlation between predictor variables does not exclude the ability to obtain a good model fit or tend to affect inferences about mean responses or predictions of new observations. However, the estimated regression coefficients tend to have large sampling variability and thus the estimated regression coefficients tend to vary widely from one sample to the next when predictor variables are highly correlated (Kutner et al., 2005). Variable inflation factors (VIF) are estimated to assess the strength and sources of collinearity among the variables. The higher the VIF, the more serious the multicollinearity, thus requiring correction. The three variables with the highest VIF are excluded from the second step of the regression analysis. The remaining variables were included as predictors. Lastly, an alternative third model, Model 2, is devised. The adopted strategy involved performing Belsley collinearity diagnostics (Belsley, 1991) and analysing the Pearson correlation coefficients. Belsley collinearity diagnostics consist of a two-step procedure. First, singular values of the scaled variable matrix are computed and converted into condition indices. These values represent the collinearity of combinations of variables in the dataset, through the relative size of the eignevalues of the matrix. Afterwards, the variance of the ordinary least squares estimates of the regression coefficients in terms of the singular values (variance-decomposition proportions) is computed. These values indicate the

proportion of variance for each regression coefficient (and associated variable) attributable to each condition index (eigenvalue). These identify groups of variables involved in dependencies, and the extent to which the dependencies degrade the regression. Afterwards, an analysis of the Pearson correlation coefficients is made. If two variables have a Pearson correlation coefficient above 0.75, one of them is dropped. This process is repeated until only variables with correlation coefficients (between them) below 0.75 existed. These final variables are then included as predictors in the stepwise regression.

2.7 Model Validation

The data of the remaining 4 participants not chosen to integrate the model building (2 females and 2 males, age: 23.8 ± 1.3 years, height: 1.73 ± 0.11 m, weight: 65.5 ± 14.1 kg) are used to validate the regression models. Lastly, the model developed by Xu et al. (2014a) that only included thoracohumeral angles and the model developed by Grewal and Dickerson (2013) were applied to this work's validation dataset. This was made to assess how well the regression equations developed by other authors, which exclude thoracohumeral negative planes of elevation, estimate the wider-ranging dataset of joint rotations contained in the present work.

3 RESULTS AND DISCUSSION

3.1 Regression Equations

The following tables 3 and 4 indicate the obtained regression equations for Model 0 (M0), Model 1 (M1) and Model (3). All the equations are in Wilkinson notation (Wilkinson et al., 1973). In this notation, each term is multiplied by the coefficient associated with it. A colon (:) between two variables indicates the interaction (product) of the two independent variables. The intercept is added to all the other variables predictors as its value, the intercept's coefficient. The joint angle is calculated in the form: Joint Rotation = Intercept's coefficient + $Term_1$ * Coefficient $_1$ + Term $_2$ * $Coefficient_2$ + … Term $_n$ * Coefficient $_n$, where the terms 1 to *n* are the terms listed in each row of the following tables and the coefficients 1 to *n* are their corresponding coefficients.

Table 3: Regression equations obtained for the scapular retraction/protraction (ST1), scapular lateral/medial rotation (ST2) and scapular anterior/posterior tilt (ST3 for Model 0 (M0), Model 1 (M1) and Model 2 (M0).

Joint Rotation	Term	Coefficient
ST1(**M0**)	Intercept	37.625
	HT1	0.14212
	HT3	0.1085
ST2(**M0**)	Intercept	5.439
	HT1	0.22365
	HT2	0.60913
	HT3	0.11633
	HT1:HT2	0.0025723
	HT2:HT3	-0.00086994
	$HT2^2$	0.0022037
	$HT3^2$	0.0010033
ST3(**M0**)	Intercept	-8.6489
	HT1	0.043321
	HT2	0.1057
	HT3	0.0095627
	HT1:HT2	0.00057578
	HT2:HT3	0.0012797
	$HT1^2$	0.00061026
	$HT2^2$	0.00066838

Joint Rotation	Term	Coefficient
ST1(**M1**)	Intercept	-3584.8
	HT1	-1.4881
	HT3	-1.2679
	Age	-0.41617
	Height	3919.8
	LengthThorax	3.5065
	LengthClavicle	0.13733
	HT1:Height	0.92271
	HT3:Height	0.77326
	$HT1^2$	0.00040604
	$Height^2$	-1171.1
	$LengthThorax^2$	-0.0090076
ST2(**M1**)	Intercept	-220.25
	HT1	0.30868
	HT2	0.13334
	HT3	0.1731
	Age	0.089883
	LengthClavicle	2.8015
	HT1:HT2	0.0020497
	HT1:Age	-0.0040594
	HT2:LengthClavicle	0.0024806
	$HT2^2$	0.0012891
	$HT3^2$	0.00083255
	$LengthClavicle^2$	-0.0088142
ST3(**M1**)	Intercept	373.5
	HT1	0.22672
	HT2	0.047529
	HT3	0.0777
	Weight	-0.65702
	LengthThorax	-2.7636
	LengthClavicle	-0.1558
	LengthScapularSpine	-0.68857
	HT1:LenghtClavicle	-0.0013056
	HT2:HT3	0.0012667
	HT2:Weight	0.0038596
	HT2:LenghtThorax	0.0012819
	HT2:LenghtScapularSpine	-0.004206
	HT3:LenghtThorax	0.00071073
	HT3:LenghtScapularSpine	-0.0014355
	$HT1^2$	0.00042391
	$Weight^2$	0.0084557
	$LengthThorax^2$	0.0070335

Joint Rotation	Term	Coefficient
ST1(**M2**)	Intercept	3117.5
	HT1	0.97919
	HT3	0.5838
	Age	-74.423
	DepthThorax	-8.2565
	LenghtScapularSpine	-0.16576
	UpperArmLength	-5.7584
	HT1:Age	-0.0047428
	HT1:DepthThorax	-0.0030871
	HT3:Age	-0.0031637
	HT3:DepthThorax	0.0017992
	Age:UpperArmLength	0.21556
	$HT1^2$	0.00034112
	$DepthThorax^2$	0.015826
ST3(**M2**)	Intercept	-154.97
	HT1	-0.039031
	HT2	0.67123
	HT3	-0.092566
	Age	6.5428
	DepthThorax	0.6078
	UpperArmLength	0.033197
	HT1:Age	0.0023588
	HT2:HT3	0.0011436
	HT2:Age	-0.0032685
	HT2:UpperArmLength	-0.0016215
	HT3:DepthThorax	-0.00046138
	Age:DepthThorax	-0.029464
	$HT1^2$	0.0004699
ST2(**M2**)	Intercept	642.14
	HT1	0.25548
	HT2	1.1392
	HT3	1.2062
	Age	-19.742
	LengthScapularSpine	-0.50505
	UpperArmLength	-1.6496
	HT1:HT2	0.0013968
	HT1:HT3	-0.0013124
	HT1:Age	-0.0052936
	HT2:Age	-0.003537
	HT2:LengthScapularSpine	-0.0038282
	HT3:UpperArmLenght	-0.031106
	Age:UpperArmLenght	0.057224
	$HT1^2$	-0.00073989
	$HT2^2$	0.001318

Table 4: Regression equations obtained for the clavicular retraction/protraction (SC1) and clavicular elevation/depression (SC2) for Model 0 (M0), Model 1(M1) and Model 2 (M2).

Joint Rotation	Term	Coefficient
SC1(**M0**)	HT1	0.20188
	HT2	0.040005
	HT3	0.15876
	HT1:HT2	0.0019354
	HT1:HT3	-0.0013034
	$HT2^2$	-0.0011866
SC2(**M0**)	Intercept	-4.4813
	HT2	0.4926
	HT3	0.0012678
	HT2:HT3	-0.00066918
	$HT2^2$	0.0025672
	$HT3^2$	0.0010362

Joint Rotation	Term	Coefficient
SC1(**M1**)	Intercept	21.299
	HT1	0.409
	HT2	0.099103
	HT3	0.15257
	Gender	244.03
	Height	-80.408
	LengthClavicle	0.59722
	HT1:HT2	0.0017871
	HT1:HT3	-0.00065256
	HT1: Gender	0.095278
	HT1:LengthClavicle	-0.0017409
	HT2:Gender	0.068999
	Gender:Height	-136.23
	$HT2^2$	-0.00060118
	$HT3^2$	0.00052902
SC2(**M1**)	Intercept	-515.72
	HT2	0.065868
	HT3	-0.16164
	Age	10.288
	LengthThorax	-0.26689
	LengthClavicle	5.6162
	LenghtScapularSpine	0.56309
	HT2:LengthScapularSpine	0.0027958
	HT3:Age	0.0021178
	HT3:LengthClavicle	0.00099873
	Age:LengthClavicle	-0.075438
	$HT2^2$	0.0019164
	$HT3^2$	0.0010169
	$LengthClavicle^2$	-0.014404

Joint Rotation	Term	Coefficient
SC1(**M2**)	Intercept	1528
	HT1	0.53355
	HT2	-2.1723
	HT3	-0.14505
	Age	-0.18676
	DepthThorax	0.835
	LengthClavicle	-24.975
	LengthScapularSpine	-0.34333
	UpperArmLength	0.61038
	HT1:HT2	0.0013606
	HT1:HT3	-0.00053046
	HT1Age	-0.043227
	HT1:DepthThorax	-0.0038112
	HT1:LenghtScapularSpine	0.0053292
	HT2:DepthThorax	0.0031456
	HT2:UpperArmLength	0.042351
	H3:LenghtScapularSpine	0.0023203
	$HT2^2$	-0.0010446
	$HT3^2$	0.00050131
	$LengthClavicle^2$	0.080888
SC2(**M2**)	Intercept	315.68
	HT2	0.22318
	HT3	0.050851
	Weight	0.34562
	DepthThorax	-0.21574
	LengthClavicle	-3.4244
	HT2:DepthThorax	0.00082935
	$HT2^2$	0.0019409
	$HT3^2$	0.00098148
	$LenghtClavicle^2$	0.0098947

3.2 Analysis of Developed Models

For the first model, excluding all individual factors, the first step of the regression analysis indicated that all thoracohumeral predictors contributed to all sternoclavicular and scapulothoracic joint angles. The second step eliminated HT2 as a predictor of retraction/protraction of the scapula and HT1 as a predictor of the elevation/depression of the clavicle. The lateral/medial rotation of the scapulothoracic joint had the greatest R^2, of 0.81, while the retraction/protraction of the scapulothoracic joint had the least R^2, of 0.26. The RMSE of the model ranged between 5.26º, for the anterior/posterior tilt of the scapula, and 8.36º, for the retraction/protraction of the scapula. For the validation dataset, R^2 ranged between 0.05, for the retraction/protraction of the scapula, and 0.75 for the retraction/protraction of the clavicle, while the RMSE ranged from 5.05º, for the anterior/posterior tilt of the scapula, and 10.80º, for the lateral/medial rotation of the scapula.

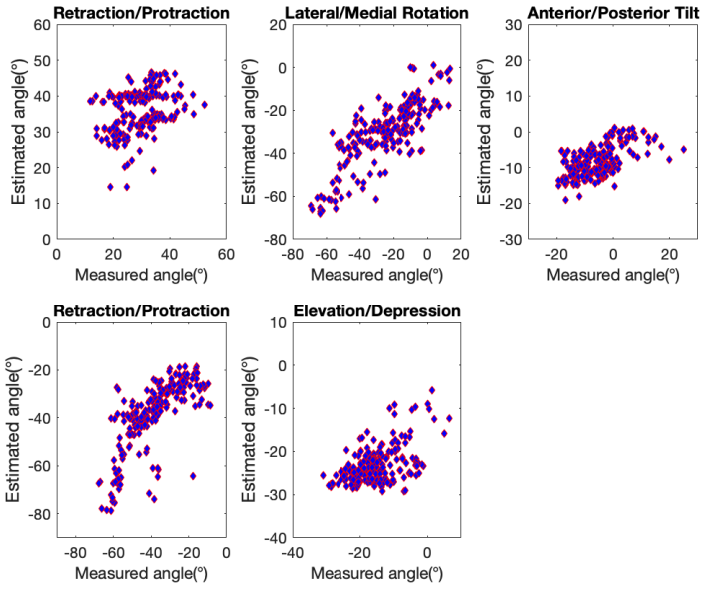

Figure 3**:** The correlation between the measured and the predicted sternoclavicular and scapulothoracic joint angles for Model 0.

Model 1 considered the three thoracohumeral angles as well as the individual factors. After the statistical processing, thorax depth, scapular length and upper arm length were the three variables with the highest VIF and were thus excluded from the second step of the regression analysis. Quadratic prediction models were obtained for all scapular and clavicular angles. The retraction/protraction of the sternoclavicular joint had the highest R^2 value of 0.86, which means that approximately 86% of the

observed variation can be explained by the model's inputs. As with Model 0, retraction/protraction of the scapulothoracic joint had the lowest R^2 value of 0.62. The RMSE of the model ranged between 3.75º for the anterior/posterior tilt of the scapula and 7.09º for lateral/medial rotation of the scapula.

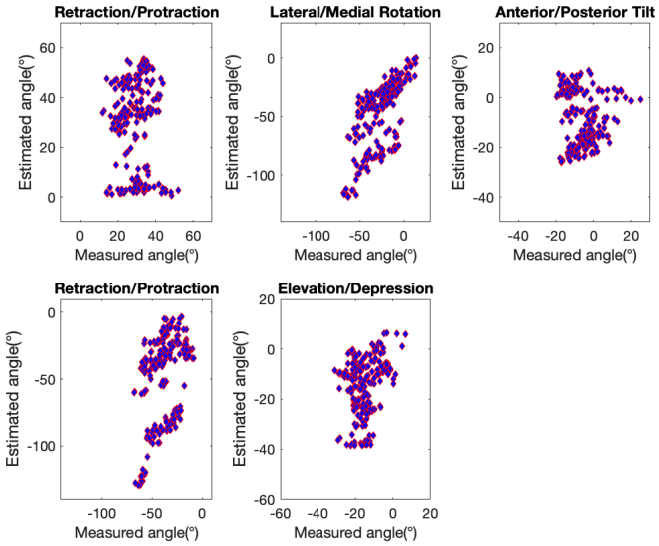

Figure 4: The correlation between measured and predicted sternoclavicular and scapulothoracic joint angles for Model 1.

Model 2 included both Belsley collinearity diagnostics (Belsley, 1991) and analysing the Pearson correlation coefficients, in order to reduce multicollinearity among variables. The first indicated all variables with the exception of the three thoracohumeral angles, i.e., all individual factors were involved in strong dependencies. Afterwards, the predictor variables selected to integrate the stepwise regression were decided following an analysis of the Pearson correlation coefficients. The only predictors with correlation coefficients (between them) below 0.75 were age, weight, scapular spine length, clavicular length, thorax depth and upper arm length, plus the three thoracohumeral angles, HT1, HT2 and HT3. Quadratic prediction models were obtained for all scapular and clavicular angles. The retraction/protraction of the sternoclavicular joint had the greatest R^2 value of 0.89, retraction/protraction of the scapulothoracic joint had the least R^2 value of 0.65. The RMSE of the model ranged between 3.60º for the anterior/posterior tilt of the scapula and 6.63º for lateral/medial rotation of the scapula.

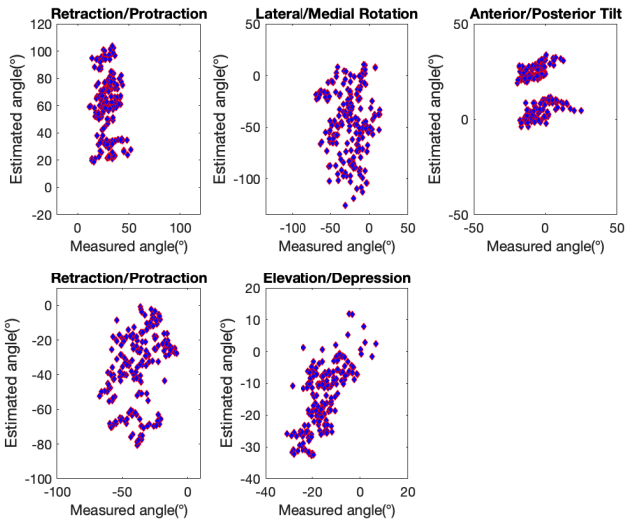

Figure 5: The correlation between the measured and the predicted sternoclavicular and scapulothoracic joint angles for Model 2.

Some differences are exhibited between the regression models computed in this study and those from past works (de Groot and

Brand, 2001; Grewal and Dickerson, 2013; Xu et al., 2014a). Xu et al. (2014a) considered the three thoracohumeral parameters significant for all joint rotations, with the exception of scapular retraction/protraction. This was not supported by this work or the work of Grewal and Dickerson (2013). Both in his work and in this study, the three thoracohumeral angles were significant predictors for all joint angles except for scapular retraction/protraction and clavicular elevation/depression. In the present study scapular retraction/protraction was only influenced by HT1 and HT3, which is in agreement with the work of Xu et al. (2014a) but opposes the findings of Grewal and Dickerson (2013), where the two significant angles were HT1 and HT2. A possible explanation for this could be the more efficient thoracohumeral discretization achieved by the present work and the one from Xu et al. (2014a). In the present work axial rotation was tracked using IMU and Xu et al. (2014a) resorted to frame stabilization. Grewal and Dickerson (2013) did not track the axial rotation configurations, which might have obscured the influence of this parameter angle. In what concerns clavicular elevation/depression both this study and the one from Grewal and Dickerson (2013) considered HT2 and HT3 as the only significant thoracohumeral predictors. All three clavicular elevation/depression regression equations obtained in this work have a squared elevation angle predictor term. This is supported by observed non-linear changes of clavicular elevation with humeral elevation (Barnett et al., 1999; Ludewig et al., 2009; McClure et al., 2001). Every sternoclavicular and scapulothoracic joint angles had, in models 1 and 2, individual factors as significant predictor variables. This agrees with Xu et al. (2014a) but opposes the findings of other previous works. In de Groot and Brand (2001), it was found that gender and anthropometry data were not significant predictors. In Grewal and Dickerson (2013), age, height, and weight were also excluded in the regression model due to lack of predictive power. Xu et al. (2014a) hypothesized that this could be a result of participant selection. In his study, the participants had a larger diversity in terms of age and weight than the participants in those previous studies, which might have contributed to less model predictability and accentuated the effect of the individual factors. All individual factors considered in this study impacted at least one of the joint rotations, with the exception of scapular length, which was always excluded by the statistical processing. Scapular length was shown to be involved in severe multicollinearity. This is in agreement with Campobasso et al. (1998) who found that the scapula could be reliably employed for the estimation of stature in forensic practice.

The models show how the inclusion of individual factors in the regression improves the fit to the data from the test group. This is possibly due to the increase in degrees of freedom (maximum number of logically independent values, which are values that are free to vary). But this inclusion has varying results when predicting the validation dataset. This is a direct consequence of the multicollinearity among the predictor variables. Multicollinearity causes the estimated regression coefficients to vary widely from one sample to the next. All in all, the inclusion of individual factors worsened the predictability of mainly clavicular retraction/protraction and, for Model 1, scapular anterior/posterior tilt. For the current model with no individual factors, the RMSE are in a similar range as those found in the works of de Groot and Brand (2001) and Xu et al. (2014a) . The inclusion of individual factors in our model reduced the computed RMSE, which were in general lower than the ones in the literature. The values of R^2 in Model 0 were higher than the ones obtained by Xu et al. (2014a). The inclusion of individual factors in our models further increased R^2.

The models applied to the validation dataset which included individual factors revealed a difference between measured and predicted values in the range of the models derived by de Groot and Brand (2001) and Xu et al. (2014a). The differences were, however, generally larger than the ones found in the work of Grewal and Dickerson (2013), especially those in Model 2. This may be due to the inclusion of a larger selection of anthropometric data in the regression models of this study, which likely increased multicollinearity problems, even when filtered through the analysis of the Variable Inflation Factors (VIF) (Model 1) and the Belsley collinearity diagnostics and Pearson correlation coefficients (Model 2). On the other hand, past regression models were built using a larger number of participants with greater diversity of age, height, weight and anthropometric data. This could explain why past models showed better predictive power in their respective validation stages, as the regression equations were computed using more diverse values of predictor variables.

Lastly, the model developed by Xu et al. (2014a) that only included thoracohumeral angles was applied to our validation dataset. The largest error was obtained for the scapular lateral/medial rotation, where the RMSE was 14.00°. The application of Model 0 to the validation dataset also resulted in the largest error for this joint angle, with RMSE = 10.80º. The RMSE obtained from the validation dataset used by Xu et al. (2014a) was the second highest presented in his work, 7.40°. The best prediction using the equations of Xu et al. (2014a) was observed for clavicular retraction/protraction ($R^2 = 0.70$). The same process was

done for the model developed by Grewal and Dickerson (2013**),** applying it to our validation dataset. The largest error was obtained for the scapular lateral/medial rotation, where the RMSE was 14.50°. It was also the angle where Model 0 presented the highest RMSE. The best prediction using the equations of Grewal and Dickerson (2013) was observed for clavicular retraction/protraction ($R^2 = 0.45$), which is in agreement with the highest R^2 found in his own work. It was also the joint angle for which the equations from Xu et al. (2014a) provided the best prediction. This shows the equations developed in these past works have moderate success predicting some of the studied joint angles for wider-ranging humeral postures, specifically those in negative elevation planes, being surpassed by the model developed over the course of this work.

3.3 Accuracy of the External Frame

All the postures, with the exception of the ones with a thoracohumeral elevation of 0°, were standardized with the aid of the external frame. This frame efficiently systematized the tracked postures. The highest angle differences occurred at the most negative elevation plane (frame defined plane of -90°) where the average angle difference between frame-defined and measured planes was 17.4°, and at the postures with the highest elevation angle (frame defined elevation angle of 160°). For this elevation angle, the average angle difference between frame-defined and measured elevation angles was 23.7°. This is a significant improvement to the work of Xu et al. (2014b) who had a lower maximum elevation angle (150°), for which average angle differences of 49.2° were found. This shows an improvement in the standardization of humeral postures even at the most extreme positions of the novel range of motion.

4 CONCLUSION

Regression equations for 3-D multiplanar shoulder rhythms were developed considering a larger envelope of arm postures than the one currently available in the literature. Past studies neglected arm postures in negative planes of elevation, which are particularly prevalent in ample upper limb motions, such as those in swimming activities. An optoelectronic tracking system complemented with the usage of inertial measurement units was used to acquire shoulder kinematics, in a series of arm postures supported by an external frame. This external frame efficiently improved the consistency of arm positioning and the comfort of subjects. A three-pointed palpatory, scapula locator, was 3-D printed to help locate the scapular anatomical landmarks during postures with significant soft tissue displacement. Overall, this work was successful in extending the regression-based 3-D shoulder rhythm equations to a wider range of arm postures. The model without individual factors showed a fit to the data in the range of the preceding study with the highest angular resolution of arm postures (Xu et al., 2014a). This allows the conclusion that an extension of the 3-D regression models to ranges of motion including negative planes of humeral elevation was possible, without compromising the models´ predictability. The impact of individual factors on the regression models requires, however, a more careful approach. The models with individual factors showed a better fit to the initial test dataset than the model without, possibly due to the increase in degrees of freedom. The model from the validation dataset showed, on the other hand, that the inclusion of individual factors in the regression has varying results when predicting the validation dataset. This can be explained by the high multicollinearity found among the predictor variables, which causes the computed regression coefficients to be very sensitive to small changes in the model. Even after a preselection of the individual factors through a statistical study, multicollinearity was still found. The anthropometrical data includes segments that are constrained by their relation in a closed chain mechanism and thus a degree of variable dependency is unavoidable. This study had important limitations. First and foremost, the subjects were selected from an homogenous group. This lack of diversity might have confounded the influence of personal factors. Additionally, the effects of force exertion on shoulder rhythm were not studied. A future study should consider these external forces in conjunction with the newly tested negative planes of humeral elevation. Another point of future interest is the definition of the body orientations. This study used Euler angles, in alignment, and to allow comparison, with the existing literature. These orientation angles are computed from a given rotation matrix by performing an inverse transformation. The inverse transformation problem has, however, two solutions for which two of the Euler angles, describe the same rotation and cannot be computed separately, and thus one degree of freedom is lost (Project, 1986). This problem can be solved using Euler parameters to parametrize the rotation matrix. It would therefore be interesting to see a 3-D regression model that studied the shoulder rhythm using as predictors thoracohumeral positions represented by these Euler parameters. This could help generalize the prediction of the shoulder rhythm from the positions of the thorax and

the arm and thus lead the way to a better understanding of the intricacies of shoulder kinematics.

References

Aiken, L. S., & West, S. G. 1991. *Multiple regression: Testing and interpreting interactions.* Sage Publications, Inc.

Barnett, N.D., Duncan, R.D.D., Johnson, G.R., 1999. The measurement of three dimensional scapulohumeral kinematics—a study of reliability. *Clinical Biomechanics***. 14**, 287–290.

Belsley, D.A. 1991. A guide to using the collinearity diagnostics. *Computer Science in Economics and Management*, **4**(1), 33-50.

Brochard, S., Lempereur, M., Remy-Neris, O. 2011. Double calibration: an accurate, reliable and easy-to-use method for 3D scapular motion analysis. *Journal of Biomechanics*. **44** (4), 751–754.

Campobasso, C.P., G. Di Vella, and F. Introna, Jr.1998. Using Scapular Measurements in Regression Formulae for the Estimation of Stature. Bollettino della Societa Italiana di Biologia Sperimentale **74**(7-8):75-82.

De Groot, J. H., & Brand, R. 2001. A three-dimensional regression model of the shoulder rhythm. *Clinical Biomechanics*, **16**(9), 735–743. https://doi.org/10.1016/S0268-0033(01)00065-1.

Gamage, S. S. H. U., & Lasenby, J. 2002. New least squares solutions for estimating the average centre of rotation and the axis of rotation. *Journal of Biomechanics*, **35**(1), 87–93.

Grewal, T. J., & Dickerson, C. R. 2013. A novel three-dimensional shoulder rhythm definition that includes overhead and axially rotated humeral postures. *Journal of Biomechanics*, **46**(3), 608–611. https://doi.org/10.1016/j.jbiomech.2012.09.028.

Hogfors, C., Peterson, B., Sigholm, G., Herberts, P. 1991. Biomechanical model of the human shoulder joint.2. The shoulder rhythm. *Journal of Biomechanics*, **24**, 699–709.

Inman, V. T., Saunders, J. B., Abbott, L.C. 1944. Observations on the function of the shoulder joint. *Journal of Bone and Joint Surgery*, **26**(1), 1-30.

Karduna, A. R., McClure, P.W., Michener, L.A., Sennett, B. 2001. Dynamic measurements of three-dimensional scapular kinematics: a validation study. *Journal of Biomechanical Engineering*, **123** (2), 184–190.

Kutner, M., Christopher, Nachtsheim, J. C., Neter, J., & Li, W. (2005). In Applied Linear Statistical Models. In *Building the regression model II: Diagnostics*.

Ludewig, P. M., Phadke, V., Braman, J. P., Hassett, D. R., Cieminski, C. J., & Laprade, R. F. 2009. Motion of the shoulder complex during multiplanar humeral elevation. *Journal of Bone and Joint Surgery - Series A*, **91**(2), 378–389. https://doi.org/10.2106/JBJS.G.01483.

McClure, P. W., Michener, L. A., Sennett, B.J., Karduna, A.R. 2001. Direct 3-dimensional measurement of scapular kinematics during dynamic movements in vivo. *Journal of Shoulder and Elbow Surgery*, **10**(3), 269-277.

Meskers, C. G. M., van de Sande, M. A. J., & de Groot, J. H. 2007. Comparison between tripod and skin-fixed recording of scapular motion. *Journal of Biomechanics*, **40**(4), 941–946. https://doi.org/10.1016/j.jbiomech.2006.02.011.

Prinold, J.A., Shaheen, A.F., Bull, A.M. 2011. Skin-fixed scapula trackers: a comparison of two dynamic methods across a range of calibration positions. *Journal of Biomechanics*. **44** (10), 2004–2007.

Project, P. A. 1986. Production automation. *Data Processing*, **28**(8), 441. https://doi.org/10.1016/0011-684x(86)90434-x.

Wakimoto K., Dakeshita T., Wakimoto J., et al. 2018. Effects of triple-treatment trunk stretching on physical fitness and curvature of the spine. *Heliyon*, **4**(12), (Dec 1, 2018), e00985. doi: 10.1016/j.heliyon.2018.e00985.

Wilkinson, G., & Rogers, C. 1973. Symbolic Description of Factorial Models for Analysis of Variance. *Journal of the Royal Statistical Society. Series C (Applied Statistics),* **22**(3), 392-399. doi:10.2307/2346786.

Wu, G., van der Helm, F. C., Veeger, H. E., Makhsous, M., van Roy, P., Anglin, C., Nagels, J., Karduna, A. R., McQuade, K., Wang, X., Werner, F. W., Buchholz, B. 2005. ISB recommendation on definitions of joint coordinate systems of various joints for the reporting of human joint motion. Part II. Shoulder, elbow, wrist and hand. *Journal of Biomechanics*, **38**(5), 981-992.

Van Andel, C., van Hutten, K., Eversdijk, M., Veeger, D. J., & Harlaar, J. 2009. Recording scapular motion using an acromion marker cluster. *Gait and Posture*, **29**(1), 123–128. https://doi.org/10.1016/j.gaitpost.2008.07.012.

Xu, X., Lin, J. hua, & McGorry, R. W. 2014a. A regression-based 3-D shoulder rhythm. *Journal of Biomechanics*, **47**(5), 1206–1210. https://doi.org/10.1016/j.jbiomech.2014.01.043.

Xu, X., McGorry, R. W., & Lin, J. hua. 2014b. The accuracy of an external frame using ISB recommended rotation sequence to define shoulder joint angle. *Gait and Posture*, *39*(1), 662–668. https://doi.org/10.1016/j.gaitpost.2013.08.032